

The 2010 North Atlantic Hurricane Season

A Climate Perspective

Gerald Bell¹, Eric Blake², Todd Kimberlain², Chris Landsea²,
Jae Schemm¹, Richard Pasch², Stanley Goldenberg³

¹Climate Prediction Center/NOAA/NWS/NCEP

²National Hurricane Center/NOAA/NWS/NCEP

³Hurricane Research Division/NOAA/OAR/AOML

Contents:

1. 2010 Seasonal Activity	pp. 1-2
2. Storm Tracks and Landfalls	pp. 2-3
3. Atlantic Sea Surface Temperatures	pp. 4-5
4. Atmospheric Circulation	pp. 5-7
5. Links to Global Climate Patterns	pp. 7-8
a. The Tropical Multi-Decadal Signal	pp. 7-8
b. La Niña	p. 8
6. Summary	pp. 8-9
7. References	p. 9

1. 2010 Seasonal Activity

The Atlantic hurricane season lasts from June through November, with August-October (ASO) typically being the peak months of the season. The 2010 Atlantic hurricane season produced 19 named storms, of which 12 became hurricanes and five became major hurricanes (Cat. 3-5) (Fig. 1). All but two named storms formed during ASO. The 1950-2000 seasonal averages are eleven named storms, six hurricanes, and two major hurricanes.

Recently, Landsea et al. (2010) indicated that because of improved monitoring and analysis of weak, short-lived tropical cyclones in the last decade, the climatological averages since 1950 may have a low bias of about two tropical storms per year – giving a more realistic climatology value of about 13 named storms per

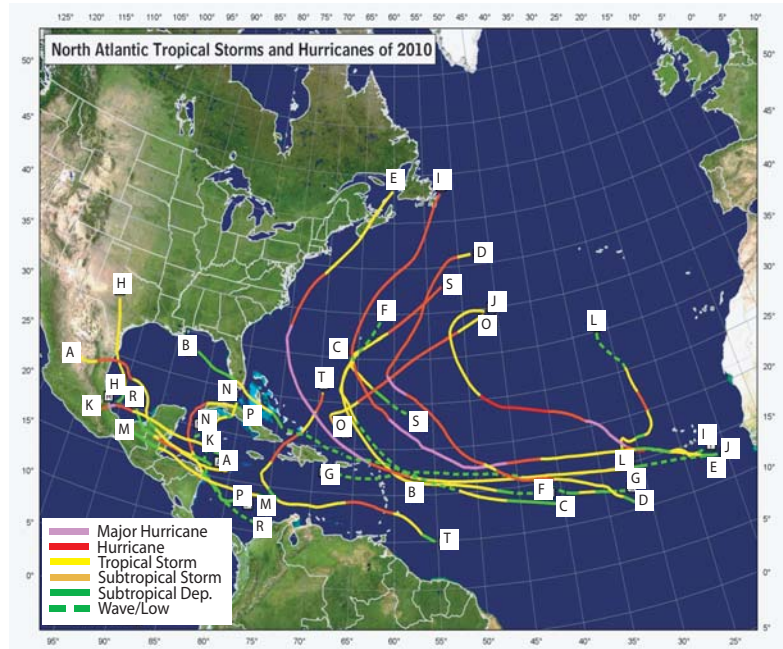


Fig. 1. Tracks of Atlantic named storms during 2010. Storm intensity is color-coded as indicated. Letters correspond to the first initial of the storm name.

year.

The 2010 seasonal Accumulated Cyclone Energy (ACE) value (Bell et al. 2000) was $166.3 \times 10^4 \text{ kt}^2$, which corresponds to 190% of the 1950-2000 median value (Fig. 2). This places 2010 as the tenth most active season since 1950.

NOAA classifies the 2010 season as “above normal,” as defined in http://www.cpc.ncep.noaa.gov/products/outlooks/background_information.shtml. NOAA’s hurricane season outlooks were issued in both late May and early August. Both outlooks indicated a high likelihood of an above-normal season, and suggested it could be one of the more active seasons on record (See an archive of NOAA seasonal outlooks at <http://www.cpc.ncep.noaa.gov/products/outlooks/hurricane-archive.shtml>).

This year also marks the ninth hyperactive season (ACE > 175% of the median) since the high activity era for Atlantic hurricanes began in 1995 (Goldenberg et al. 2001). By comparison, no hyperactive seasons occurred during the preceding 24 year period (1971-1994), which is a low activity era in the Atlantic Basin.

As is typical of very active seasons, conditions for tropical cyclone formation and intensification during 2010 were exceptionally conducive within the Main Development Region (MDR), which encompasses the Caribbean Sea and tropical Atlantic Ocean between 9.5°N and 21.5°N (Fig. 3). Most (14 of 19) named storms formed in the MDR, accounting for 10 of 12 hurricanes, all five major hurricanes, and 93% of the seasonal ACE value.

2. Storm Tracks and Landfalls

The Atlantic storm tracks during 2010 were

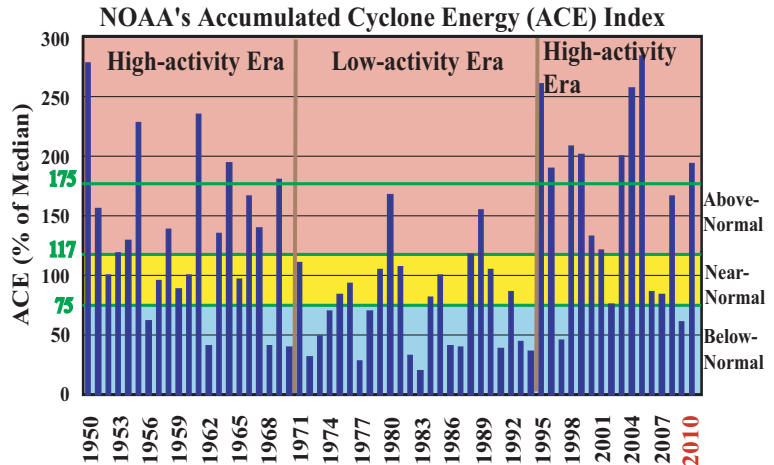


Fig. 2. NOAA’s Accumulated Cyclone Energy (ACE) index expressed as percent of the 1950-2000 median value ($87.5 \times 10^4 \text{ kt}^2$). ACE is a wind energy index that measures the combined strength and duration of the named storms. ACE is calculated by summing the squares of the 6-hourly maximum sustained wind speed (measured in knots) for all periods while the named storm has at least tropical storm strength. Pink, yellow, and blue shadings correspond to NOAA’s classifications for above-, near- and below-normal seasons, respectively. The 175% threshold for a hyperactive season is indicated. Vertical brown lines separate high-activity and low-activity eras.

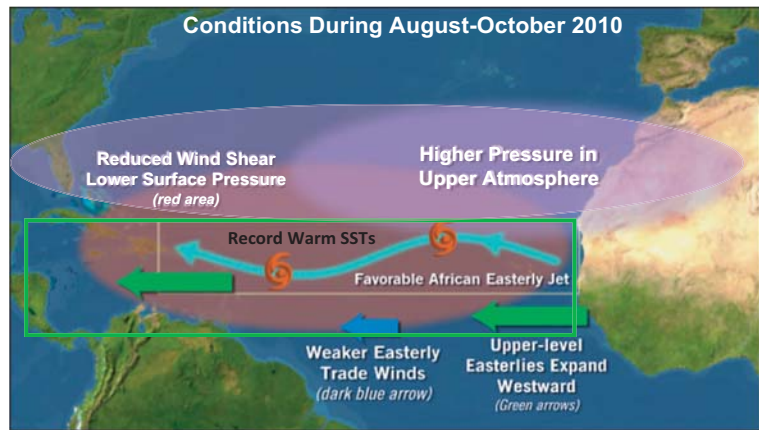


Fig. 3. Schematic depiction of atmospheric and oceanic conditions over the Atlantic basin during August-October 2010. Green box denotes the Main Development Region (MDR).

generally divided into two clusters. One cluster comprised eight storms that formed over the eastern tropical Atlantic. Five of these systems eventually became hurricanes (four became major hurricanes) and three remained tropical storms. The majority of storms in this cluster (6 of 8) tracked northward and then re-curved out to sea. The other two

storms (Earl and Igor) struck Nova Scotia and Newfoundland, respectively. This landfall ratio (25%) is close to the historical probability (29%) for a North America landfall by a storm forming over the eastern Atlantic (Kossin et al. 2010).

The second cluster of storm tracks during 2010 consisted of eleven systems that formed over or near the Caribbean Sea. This region typically sees significantly increased hurricane activity during hyperactive seasons. Many of these storms during 2010 formed near land over the western Caribbean/Mexico/Central America region. Overall, five systems in this second cluster made landfall as a tropical storm, three made landfall as a Cat. 1-2 hurricane, and one made landfall as a major hurricane.

The United States did not experience any landfalling hurricanes during 2010 (*NOAA's seasonal hurricane outlooks currently do not predict tropical storm and hurricane landfalls, nor do they indicate whether a particular region is more likely to be struck during the season.*)

This makes 2010 the most active season- and the only hyperactive season- on record to produce no U.S. hurricane landfalls. For the twelve hyperactive seasons that occurred during 1950-2009, each produced at least one U.S. landfalling hurricane, and 90% produced at least two U.S. landfalling hurricanes (red bars, Fig. 4). This rate of multiple hurricane landfalls is more than triple that (25%) associated with other above normal seasons that were not hyperactive (blue bars).

The lack of U.S. hurricane landfalls during 2010 can be attributed to several factors. First, there was a pronounced weakness over the eastern U.S. in the extensive subtropical ridge that otherwise extended from Africa to the southwestern U.S. (Fig. 5). This weakness reflected mean troughing near the U.S. east coast, and was associated with mid-level

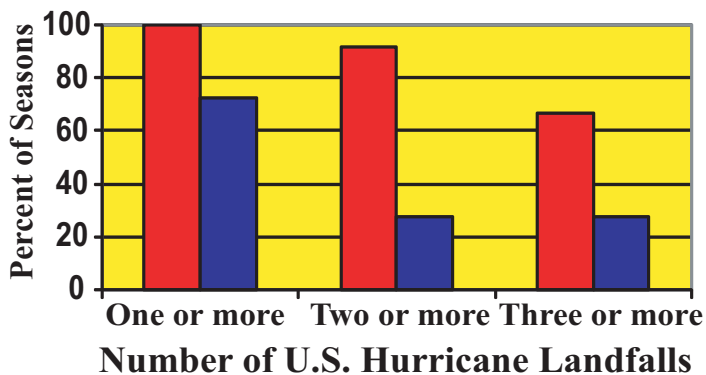


Fig. 4. Seasonal frequency (during 1950-2009) of Atlantic basin hurricanes making landfall in the United States for hyperactive seasons (Red Bars) and for above normal seasons that are not hyperactive (Blue Bars). Landfalls are based on the HURDAT data produced by the National Hurricane Center and compiled by Blake et al. (2007). Only one U.S. hurricane landfall per storm is counted.

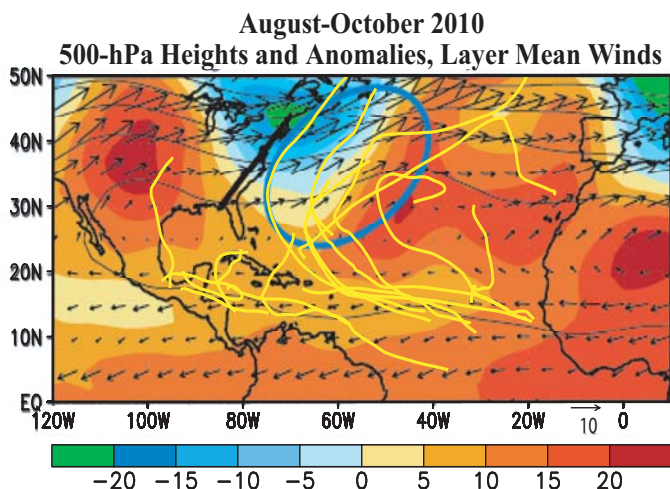


Fig. 5. ASO 2010: 500-hPa Heights (contours, m) and anomalies (shading), and layer mean vector wind (ms^{-1}) between 600 hPa – 300 hPa. Vector scale is at bottom right. Thick solid line indicates weakness in upper-level ridge, and blue circle highlights extensive southwesterly flow over the western Atlantic. ASO 2010 Atlantic named storm tracks are shown in yellow.

southwesterly flow that steered all approaching hurricanes away from the U.S.

Second, no hurricanes formed or tracked over the central and northern Gulf of Mexico, which can be attributed in part to the enhanced subtropical ridge over the Caribbean Sea. This ridge prevented storms over the Caribbean Sea from propagating northward into the central Gulf. Third, some storms formed and remained over the eastern tropical Atlantic throughout their life.

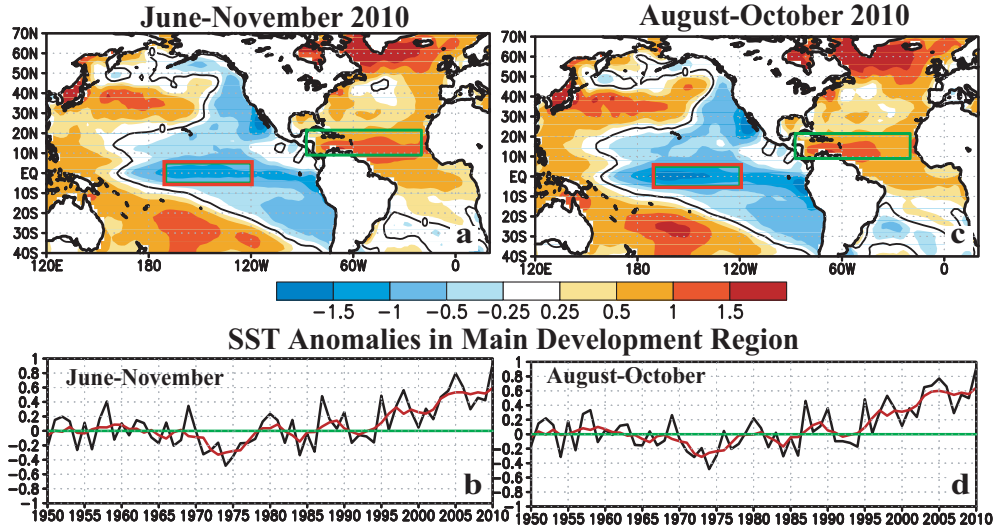


Fig. 6. (Top) SST anomalies ($^{\circ}\text{C}$) during (a) Jun-Nov 2010 and (c) Aug-Oct 2010. (Bottom) Time series of consecutive area-averaged SST anomalies in the MDR during (b) Jun-Nov, and (d) Aug-Oct. Red line shows the corresponding 5-yr running mean. Green boxes in (a, c) denote the MDR. Anomalies are departures from the ERSST-V3b (Smith et al. 2008) 1971-2000 period monthly means.

3. Atlantic Sea Surface Temperatures (SSTs)

The mean SST in the MDR during June-November was record warm (0.93°C above average) (Fig. 6a). This departure exceeds the previous record (dating back to 1854) of $+0.80^{\circ}\text{C}$ set in 2005 (Fig. 6b). The mean SST in the MDR during ASO 2010 was 0.91°C above average (Fig. 6c), which also exceeds the previous record ASO departure of $+0.77^{\circ}\text{C}$ set in 2005 (Fig. 6d).

This warmth first appeared during February-April 2010, in association with a sharply reduced strength of the anti-cyclonic gyre over the central North Atlantic (Fig. 7a) and with record weak trade winds north of the MDR (Fig. 7b).

These conditions were associated with a record negative phase of the North Atlantic Oscillation (NAO) during December-April, as measured by the 500-hPa based NAO index produced by NOAA's Climate Prediction Center (CPC, available at ftp://ftp.cpc.ncep.noaa.gov/wd52dg/data/indices/tele_index.nh). During DJF this pattern was coupled to a record negative phase of the hemispheric-scale Arctic Oscillation (AO). The monthly AO index is available at www.cpc.ncep.noaa.gov/products/precip/CWlink/daily_ao_index/monthly.ao.index.b50.current.ascii.table.)

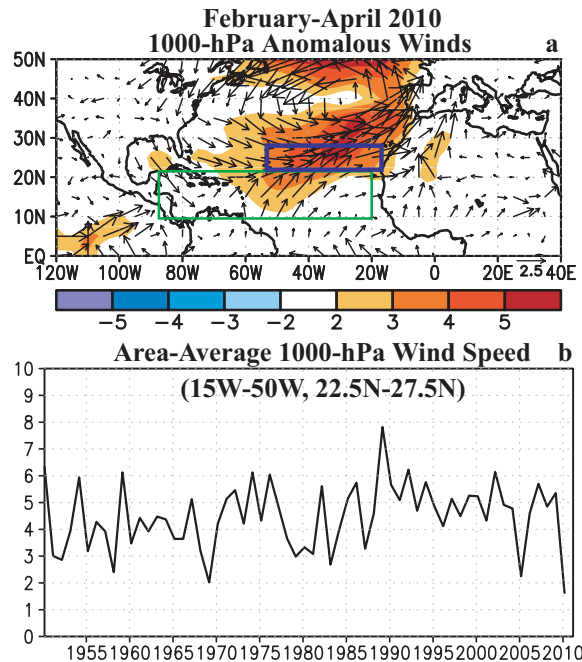


Fig. 7: February-April 2010: (a) 1000-hPa anomalous wind speed (shaded, ms^{-1}) and vector winds. (b) Time series of consecutive area-averaged total wind speed at 1000-hPa in the area bounded by 15°W - 50°W , 22.5°N - 27.5°N (blue box in panel a). Green box in (a) denotes the MDR.

The area of exceptionally weak trade winds subsequently shifted into the deep Tropics, resulting in record warm SSTs in the MDR through September (Fig. 8a). Weaker than normal trade winds and anomalously warm SSTs have generally

prevailed in the MDR since 1995, in association with the warm phase of the Atlantic Multi-decadal Oscillation (AMO, Enfield and Mestas-Nuñez 1999) and the active Atlantic phase of the tropical multi-decadal signal (Bell and Chelliah 2006, Bell et al. 2009). These conditions have been superimposed upon a weaker long-term warming trend, which some studies suggest is partly linked to anthropogenic greenhouse warming (Santer et al. 2006).

4. Atmospheric Circulation

Conditions within the MDR during 2010 reflected an inter-related set of atmospheric conditions (Fig. 3) that are typical of recent active hurri-

cane seasons (Landsea et al. 1998, Bell et al. 1999, 2000, 2004, 2006, 2009; Goldenberg et al. 2001, Bell and Chelliah 2006, Kossin and Vimont 2007). These conditions, combined with La Niña and record warm Atlantic SSTs, set the stage for the 2010 Atlantic hurricane season.

In the lower atmosphere, ASO conditions within the MDR included weaker trade winds, a deep layer of anomalous cross-equatorial flow, and below-average heights/ sea-level pressure (blue shading, Fig. 8a). Across the Atlantic basin and sub-Saharan Africa, the low-level westerly anomalies extended above 700-hPa (Fig. 8b), the approximate level of the African Easterly Jet (AEJ, Fig. 8b), and were associated with a 5° latitude northward shift of

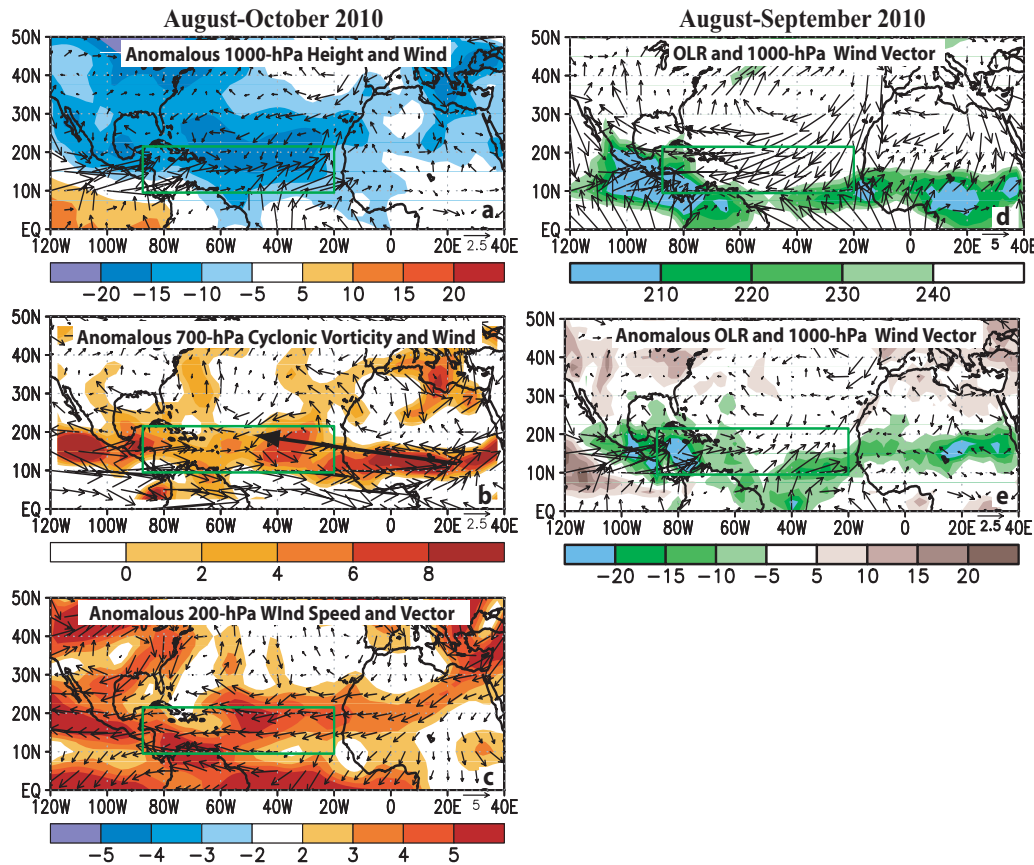


Fig. 8. Atmospheric Circulation (Left) Aug-Oct 2010 and (Right) Aug-Sep 2010: (a) Aug-Oct anomalous 1000-hPa height (shading) and vector wind (m s^{-1}), (b) Aug-Oct anomalous 700-hPa cyclonic relative vorticity (shading, $\times 10^{-6} \text{ s}^{-1}$) and vector wind, with thick solid line indicating the axis of the African easterly jet, and (c) Aug-Oct anomalous 200-hPa wind speed (shading) and vector wind. Panels (d, e) show Aug-Sep conditions: (d) total Outgoing Longwave Radiation (OLR, W m^{-2}) and 1000-hPa vector wind, (e) Aug-Sep anomalous OLR (W m^{-2}) and 1000-hPa anomalous vector wind. Green boxes denote the MDR. Vector scale is at bottom right of each panel. Circulation (OLR) anomalies are with respect to the 1971-2000 (1979-2000) period monthly means.

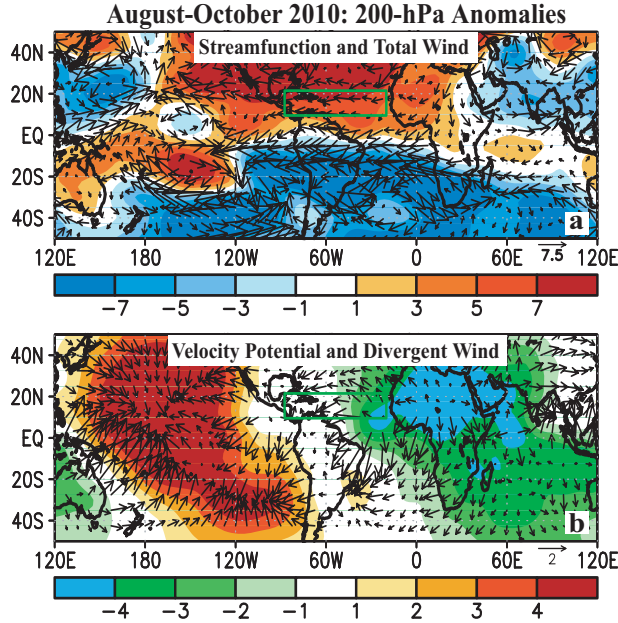


Fig. 9. Aug-Oct 2010: 200-hPa anomalies of (a) streamfunction (shading, $\times 10^6 \text{ m}^2 \text{ s}^{-1}$) and vector wind (m s^{-1}) and (b) velocity potential (shading, $\times 10^6 \text{ m}^2 \text{ s}^{-1}$) and divergent wind. Vector scales are at bottom right. Departures are with respect to the 1971-2000 period. In (a) anomalous ridges are indicated by positive values (red) in the NH and negative values (blue) in the SH. Anomalous troughs are indicated by negative values in the NH and positive values in the SH. Green boxes denote the MDR.

the AEJ core (black arrow) compared to normal.

As a result, the bulk of the African easterly wave energy (Reed et al. 1977) was often centered well within the MDR. The AEJ also featured increased cyclonic shear along its equatorward flank within the MDR (red shading), which dynamically favors stronger easterly waves, and also provides an inherent cyclonic rotation to their embedded convective cells.

An opposite pattern of wind anomalies was evident at 200-hPa, where anomalous easterly flow extended from subtropical central Africa to the eastern North Pacific (Fig. 8c). This pattern reflected a stronger and more westward extension of the tropical easterly jet, which occurred in association with an enhanced upper-level ridge that spanned the entire subtropical North Atlantic (Fig. 9a).

These conditions were accompanied by a northward shift of the Atlantic ITCZ (Inter-tropical Convergence Zone), which extended into the south-

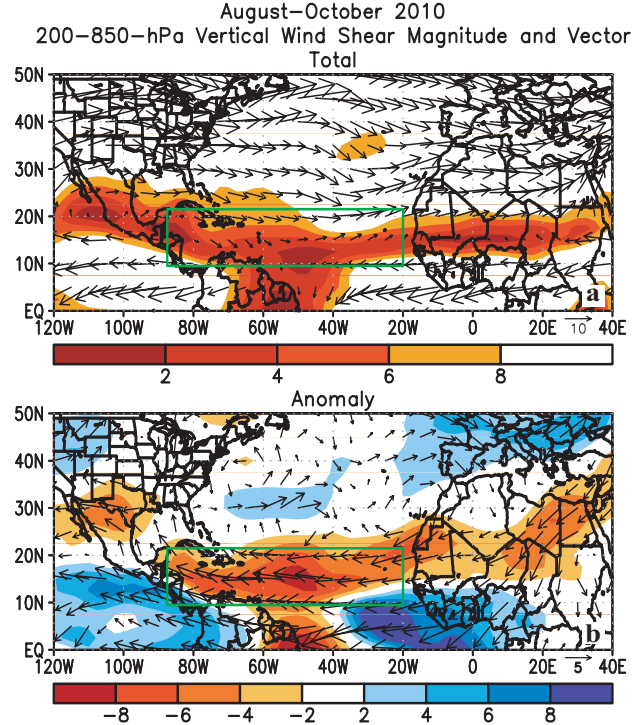


Fig. 10. Aug-Oct 2010: Vertical wind shear magnitude and vector (m s^{-1}): (a) total and (b) anomalies. Vector scale is at bottom right of each panel. Departures are with respect to the 1971-2000 period monthly means. Green boxes denote the MDR.

ern MDR during August and September, (Fig. 8d) and resulted in enhanced convection across the region (green shading, Fig. 8e). They were also associated with an amplified West African Monsoon system, as indicated by enhanced convection across the African Sahel and Sudan regions and by a large area of negative velocity potential anomalies over northern Africa (Fig. 9b).

The combination of low-level westerly and upper-easterly anomalies resulted in weak vertical wind shear (less than 8 m s^{-1}) across the entire MDR (Fig. 10a). The most anomalously weak shear spanned the central tropical Atlantic and Caribbean Sea (orange/red shading), where the total shear was less than 4 m s^{-1} .

These conditions were part of a larger-scale pattern that included increased shear across the eastern equatorial Atlantic and over the eastern tropical North Pacific (blue shading, Fig. 10b). This pattern is typical of other very active Atlantic hurricane sea-

sons (Bell and Chelliah 2006). At the same time, historically low hurricane activity prevailed across the central and eastern Pacific hurricane basins.

For the Atlantic basin, the above conditions meant that tropical storms developed primarily within the MDR from amplifying easterly waves moving westward from Africa. These systems quickly entered an extensive area of below-average pressure, deep tropical moisture, increased low-level convergence associated with the ITCZ, and increased cyclonic shear south of the AEJ core. Many of these systems then strengthened while propagating westward within the extended region of very weak vertical wind shear and often over record warm SSTs. These overall anomaly patterns have favored increased Atlantic storm formation and intensification since 1995.

5. Links to Global Climate Patterns

The regional atmospheric conditions during 2010 showed links to a combination of three climate factors. The first is the active Atlantic phase of the tropical multi-decadal signal, which reflects an inter-related set of conditions that have been conducive to increased Atlantic hurricane activity since 1995 (Bell and Chelliah 2006). The second is La Niña, which contributed to the extensive area of weak vertical wind shear and upper-level easterlies across the MDR. The third is record warm SSTs in the MDR.

(a) The Tropical Multi-Decadal Signal

Since 1995, more than two-thirds (11 of 16) of Atlantic hurricane seasons have been above normal, and only two have been below normal (Fig. 2). This elevated level of activity contrasts sharply with the preceding low-activity era 1971-94, during which one-half of the seasons were below normal and only three were above normal.

The transition to the current high activity era was associated with a phase change of the tropical multi-decadal signal, which reflects the leading modes of tropical convective rainfall variability and Atlantic SSTs occurring on multi-decadal time scales (Bell and Chelliah 2006, Bell

et al. 2007). This signal directly links low-frequency atmospheric variability across the central and eastern MDR to an east-west oscillation in anomalous convection between western Africa (Landsea and Gray 1992; Goldenberg and Shapiro 1996) and the Amazon Basin (Fig. 9).

All key features of this signal were again present during 2010, suggesting no weakening of the very conducive conditions that have prevailed throughout this Atlantic high activity era.

One key feature of the tropical multi-decadal signal seen since 1995 has been an enhanced West African monsoon system (Fig. 9b), which is associated with several of the inter-related atmospheric anomalies described in section 4 (Landsea et al.

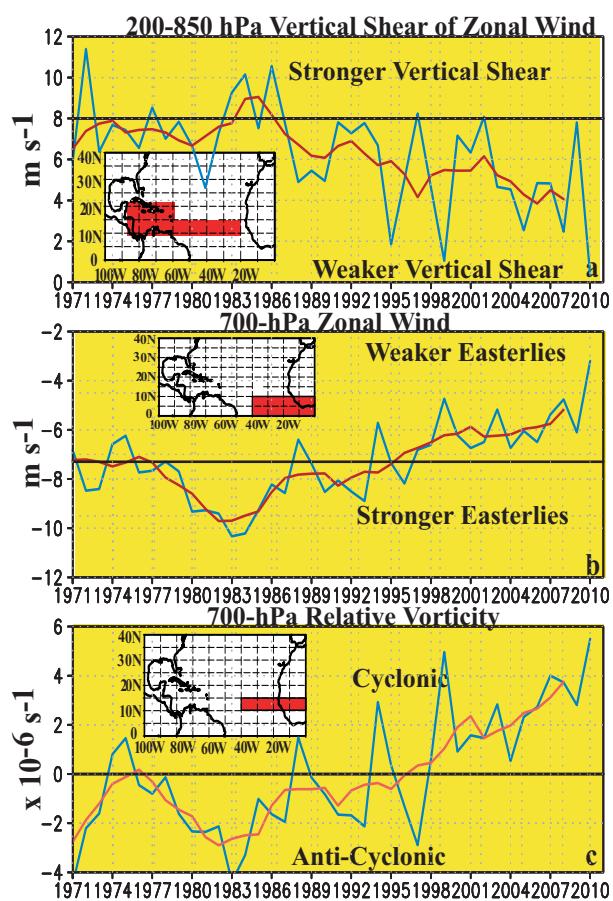


Fig. 11. Time series showing consecutive Aug-Oct values of area-averaged (a) 200-850 hPa vertical shear of the zonal wind (m s^{-1}), (b) 700-hPa zonal wind (m s^{-1}) and (c) 700-hPa relative vorticity ($\times 10^{-6} \text{ s}^{-1}$). Blue curve shows unsmoothed values, and red curve shows a 5-pt running mean of the time series. Averaging regions are shown in the insets.

1998, Bell et al. 1999, 2000, 2004, 2006, 2009; Goldenberg et al. 2001, Bell and Chelliah 2006, Kossin and Vimont 2007).

These include the enhanced low-level southwesterly flow into the West African monsoon region (Fig. 8a) and the enhanced upper-level divergent flow out of that region (Fig. 9b). They also include the stronger upper-level ridges over the eastern MDR and across the subtropical South Atlantic (Fig. 9a), along with the stronger and westward extended tropical easterly jet.

Accompanying these conditions, the vertical wind shear (Fig. 11a) and 700-hPa zonal winds (Fig. 11b) remained much weaker in critical parts of the MDR compared to the preceding low activity era, and the 700-hPa relative vorticity remained cyclonic across the southern MDR rather than anticyclonic (Fig. 11c).

b. La Niña

ENSO has long been known to affect Atlantic hurricane seasons through a combination of vertical shear and atmospheric stability variations (Gray 1984, Tang and Neelin 2004). According to the CPC, La Niña developed during July 2010 (Fig. 6a), and was a moderate-strength event during ASO.

The 200-hPa velocity potential and divergent wind anomalies across the tropical Pacific Ocean during ASO were consistent with La Niña (Fig. 9b), as was the overall zonal wave-1 pattern of 200-hPa streamfunction anomalies in the subtropics of both hemispheres (Fig. 9a) (Bell and Chelliah 2006). This pattern, which included anticyclonic streamfunction anomalies over the North Atlantic Basin and Africa, reinforced that associated with the active Atlantic phase of the tropical multi-decadal signal and resulted in the enhanced subtropical ridge extending across the entire MDR.

Also within the western MDR, typical La Niña impacts during ASO included the anomalous upper-level easterly winds and decreased vertical wind shear noted previously. These conditions acted to expand westward the anomalously low shear associated with the tropical multi-decadal signal.

6. Summary

2010 marks the eleventh above-normal Atlantic hurricane season since 1995. During 1995-2010, seasons have averaged almost 15 named storms, 8 hurricanes and 4 major hurricanes, with an ACE value of 162% of the median. This activity is similar to the previous high-activity era 1950-1970, when seasons averaged 6.5 H and 3.3 MH, with an ACE value of 136% of the median. These numbers are much higher than those observed during the low-activity era 1971-1994, when seasons averaged 5 H and 1.5MH, with an ACE value of only 75% of the median.

The above normal 2010 Atlantic hurricane activity reflected an inter-related set of atmospheric and oceanic conditions that is known to produce very active seasons. Within the MDR, these key conditions included weaker easterly trade winds, lower surface pressure, stronger tropical easterlies and an enhanced ridge at 200-hPa, reduced vertical wind shear, a very conducive structure and position of the 700-hPa African Easterly Jet, deep tropical moisture, and warmer SSTs.

Over the central and eastern MDR, these conditions have generally been in place since 1995 (Bell et al. 1999-2008), and are similar to those observed during the 1950s-1960s. They are coupled to an exceptionally strong West African monsoon system and above-average SSTs across the MDR. Their presence can be largely accounted for by the active Atlantic phase of the tropical multi-decadal signal.

La Niña, another significant climate factor, developed during July 2010 and was of moderate-strength event during ASO. Its impacts reinforced those associated with the tropical multi-decadal signal, resulting in an enhanced subtropical ridge and exceptionally weak vertical wind shear across the entire MDR.

These atmospheric conditions occurred in association with record warm SSTs in the MDR. This record warmth developed early in the year in response to a dramatic weakening of the mean anticyclonic gyre over the central Atlantic, and to record weak trade winds in the area immediately north of

the MDR.

The net result of the above climate patterns was that many Atlantic named storms formed from African easterly waves within the MDR. Many of these systems subsequently strengthened as they moved westward within the extended region of very weak vertical wind shear and record warm SSTs.

This is a classic scenario for tropical storm formation and amplification, and it is seen routinely during active seasons and high-activity eras. Such a scenario has favored increased Atlantic storm activity since 1995. NOAA's prediction for an above-normal 2010 season reflected an accurate forecast of these conditions.

Historically, the above conditions also greatly increase the hurricane activity in the region around the Caribbean Sea, as was seen this year. Similar conditions also greatly increase the probability of hurricane landfalls in the United States. However, this region was spared from hurricane landfalls during 2010, largely in response to a persistent mid-level trough over the eastern United States.

7. References

- Bell, G. D., and co-authors, 1999: Climate Assessment for 1998. *Bull. Amer. Meteor. Soc.*, **80**, S1-S48.
- Bell, G. D., and co-authors, 2000: The 1999 North Atlantic Hurricane Season: A Climate Perspective. *State of the Climate in 1999. Bull. Amer. Meteor. Soc.*, **86**, S1-S68.
- Bell, G. D., and co-authors 2004: The 2003 North Atlantic Hurricane Season: A Climate Perspective. *State of the Climate in 2003*. A. M. Waple and J. H. Lawrimore, Eds. *Bull. Amer. Meteor. Soc.*, **85**, S1-S68.
- Bell, G. D., and co-authors 2006: The 2005 North Atlantic Hurricane Season: A Climate Perspective. *State of the Climate in 2005*. A. M. Waple and J. H. Lawrimore, Eds. *Bull. Amer. Meteor. Soc.*, **86**, S1-S68.
- Bell, G. D., and co-authors 2009: The 2008 North Atlantic Hurricane Season: A Climate Perspective. *State of the Climate in 2008*. A. M. Waple and J. H. Lawrimore, Eds. *Bull. Amer. Meteor. Soc.*, **87**, S1-S68.
- Bell, G. D., and M. Chelliah, 2006: Leading tropical modes associated with interannual and multi-decadal fluctuations in North Atlantic hurricane activity. *J. Climate*, **19**, 590-612.
- Blake, E., E. N. Rappaport, and C. W. Landsea, 2007: The deadliest, costliest, and most intense United States tropical cyclones from 1851 to 2006. NOAA Technical Memorandum NWS TPC-5, NOAA National Hurricane Center. Dept. of Commerce (Available at http://www.nhc.noaa.gov/Deadliest_Costliest.shtml).
- Chelliah, M., and G. D. Bell, 2004: Tropical multi-decadal and interannual climate variations in the NCEP/NCAR Reanalysis. *J. Climate*, **17**, 1777-1803.
- Enfield, D. B., and A. M. Mestas-Núñez, 1999: Multi-scale variabilities in global sea surface temperatures and their relationships with tropospheric climate patterns. *J. Climate*, **12**, 2719-2733.
- Goldenberg, S. B., C. W. Landsea, A. M. Mestas-Núñez, and W. M. Gray, 2001: The recent increase in Atlantic hurricane activity: Causes and implications. *Science*, **293**, 474-479.
- Goldenberg, S. B., and L. J. Shapiro, 1996: Physical mechanisms for the association of El Niño and West African rainfall with Atlantic major hurricane activity. *J. Climate*, **11**, 1169-1187.
- Gray, W. M., 1984: Atlantic seasonal hurricane frequency: Part I: El Niño and 30-mb quasi-biennial oscillation influences. *Mon. Wea. Rev.*, **112**, 1649-1668.
- Kossin, J. P., and D. J. Vimont, 2007: A more general framework for understanding Atlantic hurricane variability and trends. *Bull. Amer. Meteor. Soc.*, **88**, 1767-1781.
- Kossin, J. P., S. J. Camargo, and M. Sitkowski: Climate modulation of North Atlantic hurricane tracks. *J. Climate*, **23**, 3057-3076.
- Landsea, C. W., and W. M. Gray, 1992: The strong association between Western Sahel monsoon rainfall and intense Atlantic hurricanes. *J. Climate*, **5**, 435-453.
- Landsea, C. W., G. D. Bell, W. M. Gray, and S. B. Goldenberg, 1998: The extremely active 1995 Atlantic hurricane season: Environmental conditions and verification of seasonal forecasts. *Mon. Wea. Rev.*, **126**, pp. 1174-1193.
- Landsea, C. W., G. A. Vecchi, L. Bengtsson, and T. R. Knutson, 2010: Impact of duration thresholds on Atlantic tropical cyclone counts. *J. Climate*, **23**, 2508-2519.
- Reed, R. J., D. C. Norquist, and E. E. Recker, 1977: The structure and properties of African wave disturbances as observed during Phase III of GATE. *Mon. Wea. Rev.*, **105**, 317-333.
- Santer, B. D., and co-authors, 2006: Forced and unforced ocean temperature changes in Atlantic and Pacific tropical cyclogenesis regions. *PNAS*, **103**, 13905-13910.
- Smith, T. M., R. W. Reynolds, T. C. Peterson, and J. Lawrimore, 2008: Improvements to NOAA's historical merged land-ocean surface temperature analysis (1880-2006). *J. Climate*, **21**, 2283-2296.
- Tang, B. H., and J. D. Neelin, 2004: ENSO influence on Atlantic hurricanes via tropospheric warming. *Geophys. Res. Lett.*, **31**, L24204, doi:10.1029/2004GL021072.